Binary self-assembled monolayers

Katsouras, Ilias; Geskin, Victor; Kronemeijer, Auke J.; Blom, Paul W. M.; de Leeuw, Dago M.

Published in:
Organic Electronics

DOI:
10.1016/j.orgel.2011.02.018

Publication date:
2011

Organic Electronics 12 (2011) 857–864

Contents lists available at ScienceDirect

Organic Electronics

journal homepage: www.elsevier.com/locate/orgel

Binary self-assembled monolayers: Apparent exponential dependence of resistance on average molecular length

Ilias Katsouras [a], Victor Geskin [b], Auke J. Kronemeijer [a], Paul W.M. Blom [a,c], Dago M. de Leeuw [a,d,*]

[a] Molecular Electronics, Zernike Institute for Advanced Materials, University of Groningen, Nijenborgh 4, NL-9747 AG Groningen, The Netherlands
[b] Service de Chimie des Matériaux Nouveaux, Université de Mons, Place du Parc 20, B-7000 Mons, Belgium
[c] TNO Holst Centre, 5605 KN Eindhoven, The Netherlands
[d] Philips Research Laboratories, High Tech. Campus 4, NL-5656 AE Eindhoven, The Netherlands

ARTICLE INFO

Article history:
Received 12 November 2010
Received in revised form 4 February 2011
Accepted 21 February 2011
Available online 5 March 2011

Keywords:
Alkanethiols
Electrical transport
Mixed monolayers
Molecular junction
Self-assembly

ABSTRACT

We investigate the electrical transport through mixed self-assembled monolayers of alkanemonothiols and alkanedithiols in large-area molecular junctions. To disentangle the role of the molecular length and the interfacial composition, monothiol–monothiol, dithiol–dithiol, and monothiol–dithiol binary combinations are studied. In all cases, we find that the resistance of these *mixed* SAMs appears to depend exponentially on the *average* number of carbon atoms, thus resembling *monocomponent* SAMs, whose resistance is known to depend exponentially on molecular length. However, in monocomponent SAMs this behavior has a single-molecule tunneling origin, which is not directly relevant for mixtures. Furthermore, in certain mixed SAMs the resistance *decreases* with *increasing* average layer thickness (the case of monothiol–dithiol systems). We suggest an explanation for the observed dependence of the resistance in the mixed SAMs on their composition within an equivalent circuit model based on a simple assumption concerning their microdomain structure. The simulated dependence is non-exponential but leads to a good agreement between calculated and measured resistances with only two fit parameters.

1. Introduction

Molecules self-assembled in monolayers [1] (SAM) are used extensively to control macroscopic interfacial phenomena such as wetting, adhesion, friction and charge injection [2]. The properties can be tuned by using mixed monolayers where interfacial gradients are created by adjusting the chemical composition. Mixed SAMs also provide a means for incorporating single molecules that themselves do not readily self-organize. This has been applied in molecular electronics where individual molecules embedded in an insulating matrix have been addressed with scanning probe techniques [3]. The ultimate target is to use mixed SAMs as electronic components in molecular integrated circuits. Here we study the influence of composition on the electrical characteristics of binary ensembles of molecules. We use the previously developed technology of large-area molecular junctions, a highly reproducible molecular electronic test-bed with a yield of almost unity [4]. Here, a SAM is formed on a gold bottom electrode inside a photolithographically defined vertical interconnect (via) in photoresist. The conductive polymer poly(3,4-ethylenedioxythiophene)-poly(styrenesulfonate), abbreviated as PEDOT:PSS, is spincoated on top of the SAM to fabricate the top electrode. Direct evaporation of metals on SAMs leads to short-circuit formation due to filamentary growth of metal particles [5]. The PEDOT:PSS protects the SAM when the gold top electrode is thermally evaporated and, thereby, prevents short-circuit formation. The technology is suitable for up-scaling and integration [6]. More than 20,000 molecular junctions were fabricated simultaneously on a single 150 mm wafer in a semi-automated process.

* Corresponding author at: Philips Research Laboratories, High Tech. Campus 4, NL-5656 AE Eindhoven, The Netherlands.
E-mail address: Dago.de.Leeuw@philips.com (D.M. de Leeuw).

1566-1199/$ - see front matter © 2011 Elsevier B.V. All rights reserved.
doi:10.1016/j.orgel.2011.02.018

The electrical transport through SAMs of alkanemonothiols with a methyl end group (–CH_3), and alkanedithiols with a thiol end group (–SH), has been reported previously [4,6]. Alkanedithiols with a length of *N* carbon atoms (HS–C_NH_{2N}–SH) are abbreviated as *CN*DT and alkanemonothiols (C_NH_{2N+1}–SH) as *CN*MT. The transport mechanism is nonresonant tunneling. The transmission of a junction can be modeled with a multi-barrier tunnel [7] model yielding for the resistance of a single molecule, *R*, at low bias:

$$R = \frac{h}{2e^2}T^{-1} = 12.9\ k\Omega T_{\mathrm{Au-S}}^{-1}T_{mol}^{-1}T_{SAM\ PEDOT}^{-1} \quad (1)$$

where *h* is Planck constant, *e* is the elementary charge, *T* is the overall transmission probability and where $T_{\mathrm{Au-S}}$, T_{mol} and $T_{SAM\ PEDOT}$ are the transmission probabilities for the gold–sulfur bottom contact, the molecule itself and the SAM/PEDOT:PSS top contact, respectively. Rewriting in practical terms yields:

$$R = 12.9\ k\Omega r_{\mathrm{Au-S}}r_{mol}r_{SAM\ PEDOT} \quad (2)$$

where $r_{\mathrm{Au-S}}$, r_{mol} and $r_{SAM\ PEDOT}$ are dimensionless resistance contribution factors accounting for the resistance contribution of the bottom contact, the molecule and the top contact, respectively. The molecule contribution is given by $r_{mol} \sim exp(\beta n)$, where β is the decay coefficient and *n* the number of carbon atoms in the backbone. Note that the resistance behavior of the PEDOT:PSS layer itself in a junction is nontrivial [8], and this can hold for the $r_{SAM\ PEDOT}$ contribution. Nevertheless, for a *monocomponent* SAM junction the $r_{SAM\ PEDOT}$ factor is constant and the dependence of the resistance on molecular length is found exponential [4,6,9]. This dependence derives from the r_{mol} *single-molecule* term, as long as the overall resistance is dominated by the molecule. The SAM junction resistance is then given by the single molecule resistance divided by the grafting density, under the plausible assumption that cooperative effects can be disregarded.

What about *mixed* SAMs? To investigate the contribution of both the length of the molecule and the nature of the end group we systematically studied the electric resistance of binary mixed monolayers of alkanemonothiols and alkanedithiols. First we kept the end group constant in the series of mixed monothiols and mixed dithiols, varying only the length of the molecule. Subsequently we investigated mixed SAMs of an alkanemonothiol and an alkanedithiol. In this case, both the length of the molecule as well as the interfacial composition are varied.

2. Results and discussion

2.1. "Walking along the lines"

The simplest binary SAM in terms of molecular interactions is a mixture of alkanemonothiols, in which the chemical composition of the end group is similar to that of the main chain. Let us focus on the mixed monolayers of C12MT and C18MT. In Fig. 1 the normalized resistance, *RS*, is presented on a semi-logarithmic scale as a function of the mole fraction of C18MT in the SAM solution. Each data point represents the average value of about 40 junctions. The data can be fitted with a straight line in semi-logarithmic coordinates that might indicate an exponential dependence of the normalized resistance on the composition in the SAM solution. Note that the segregation coefficient was verified to be unity, meaning that the composition of the SAM is the same as that of the solution (see Section 4). The chemical structures of the end points are schematically depicted in Fig. 1. A variation in composition translates as a linear variation in average layer thickness. Fig. 1 shows that the resistance increases with layer thickness exponentially.

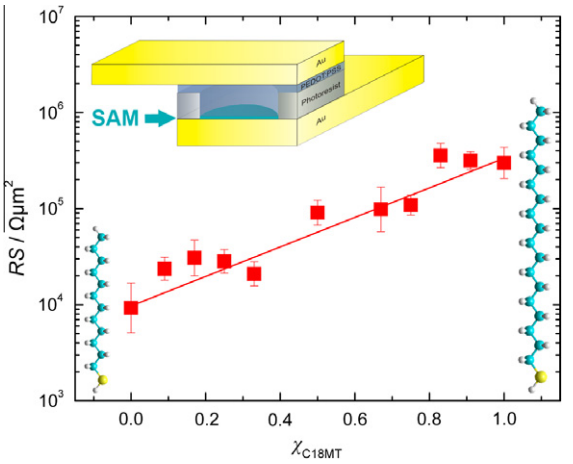

Fig. 1. Normalized resistance, *RS*, of binary mixed SAMs of C12 and C18 monothiols (C12MT and C18MT), as a function of mole fraction of C18MT in solution, χ_{C18MT}. The solid red line represents an exponential fit to the data. The inset shows a schematic cross section of the junction. The chemical structures of the end points are included to illustrate that the resistance increases with increasing layer thickness. (For interpretation of the references to colour in this figure legend, the reader is referred to the web version of this article.)

Next we turn to the resistance of a series of mixed monothiol–dithiol monolayers, namely C17MT with the dithiol C12DT. In this series both the average thickness and the interfacial composition are varied simultaneously. The normalized resistance is presented in Fig. 2 on a semi-logarithmic scale as a function of the mole fraction of C17MT in solution. Each data point represents the average value over about 20 junctions. As in the case of the mixed monothiols we observe that the normalized resistance appears to depend exponentially on composition. However, the dithiol, which is the shortest of the two molecules, has a higher resistance in monocomponent SAM than the monothiol, which is longer (their chemical structures are schematically depicted in Fig. 2). Therefore, Fig. 2 unambiguously shows that the resistance of the mixed C12DT–C17MT SAM decreases with increasing average layer thickness.

To complete this study, we fabricated all the binary monolayers of four components, *viz.* two alkanemonothiols C17MT and C20MT and two alkanedithiols C12DT and C16DT, except for the C12DT–C20MT mixed SAM. In this latter system, the big difference in the number of carbons is expected to lead to a non-unity segregation factor due to preferential adsorption [10,11]. The normalized resistances are presented in Fig. 3 on a semi-logarithmic scale

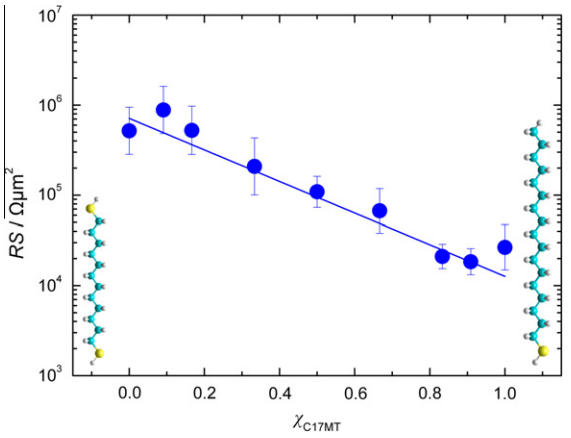

Fig. 2. Normalized resistance, *RS*, of binary mixed SAMs of C12 dithiol and C17 monothiol (C12DT and C17MT), as a function of mole fraction of C17MT in solution, χ_{C17MT}. The solid blue line represents an exponential fit to the data. The chemical structures of the end points are included to illustrate that the resistance *decreases* with *increasing* layer thickness. (For interpretation of the references to color in this figure legend, the reader is referred to the web version of this article.)

as a function of average number of atoms, as calculated from the mole fraction in solution assuming a segregation coefficient of unity. The resistances of all binary SAMs can be fitted with straight lines that might indicate an exponential dependence on the average number of atoms.

The constructed resistance diagram of Fig. 3 shows a trapezoidal correlation. The mixed monothiol C17MT–C20MT SAM and the mixed dithiol C12DT–C16DT SAM exhibit the same slope, yielding parallel lines. Throughout each of these two series, the contributions to the resistance from the top and bottom contacts are constant. The resistance changes only due to a different number of carbon atoms. The contribution of the top contact is reflected in

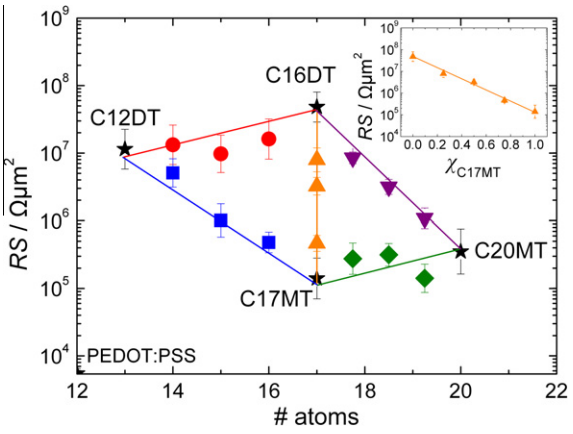

Fig. 3. Geometric resistance diagram showing a trapezoidal correlation. Normalized resistance, *RS*, of all binary mixed SAMs based on the end points C12DT, C16DT, C17MT and C20MT, as a function of average number of atoms. The fully drawn curves are a guide to the eye. The inset shows the normalized resistance of the C16DT–C17MT mixed SAMs as a function of the mole fraction of C17MT in solution. The vertical axis starts at $5 \times 10^3\ \Omega\,\mu m^2$, the value for the corresponding PEDOT:PSS only junction.

the series C16DT–C17MT. The average number of atoms in the mixed SAM is constant, while the interfacial composition is varied. The resistance systematically varies with composition over more than two orders of magnitude. The simultaneous effect of molecular length and nature of the end group is observed along the C12DT–C17MT and C16DT–C20MT lines. For both these series an apparently exponential dependence on the average number of atoms is found. The slope, however, is different because the change in the number of atoms at the end points is different; hence the corresponding lines in the trapezoid are not parallel.

2.2. Discussion

As a matter of fact, the experimental results leading to the diagram in Fig. 3 are quite puzzling. The first hypothesis to consider is that in a mixed SAM the overall resistance is given by the resistance of all its constituent individual molecules connected in parallel, i.e. as in a monocomponent SAM. It is easy to show that the behavior this hypothesis predicts contradicts experiment. Indeed, addition of significantly more conductive molecules would quickly reduce the resistance of a mixed SAM already when their fraction is low, because they would act as "shorts". On the other hand, a low share of less conductive molecules has no spectacular effect. The dependence of resistance on composition simulated in Figs. 4 and 5 is far from both the experimental points and from the straight line in semilogarithmic coordinates. We are forced to conclude that not every molecule in the mixed SAM carries current fully and independently.

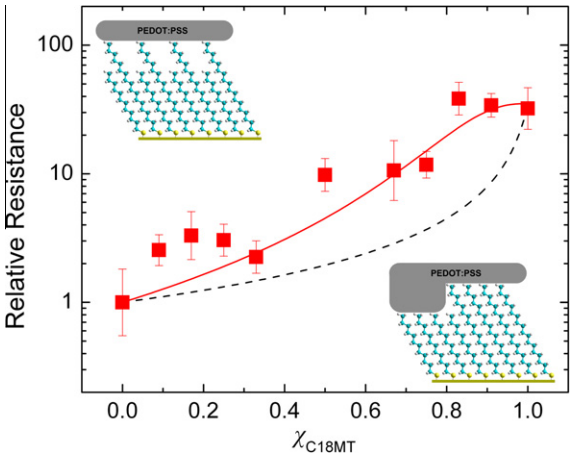

Fig. 4. Relative resistance of binary mixed SAMs of C12 and C18 monothiols (C12MT and C18MT), as a function of mole fraction of C18MT in solution, χ_{C18MT}, taken from Fig. 1 and normalized to the end point C12MT. The insets show the two cases of the mixed SAM microstructure. The top left depicts intermixing and the bottom right inset depicts phase separation. The dashed black line is calculated assuming that all the molecules of each component have the same resistance equal to their resistance in their respective monocomponent SAMs and are connected in parallel in the mixed SAMs. The solid red line is calculated by parameterization of the microstructure using Eq. (3). (For interpretation of the references to colour in this figure legend, the reader is referred to the web version of this article.)

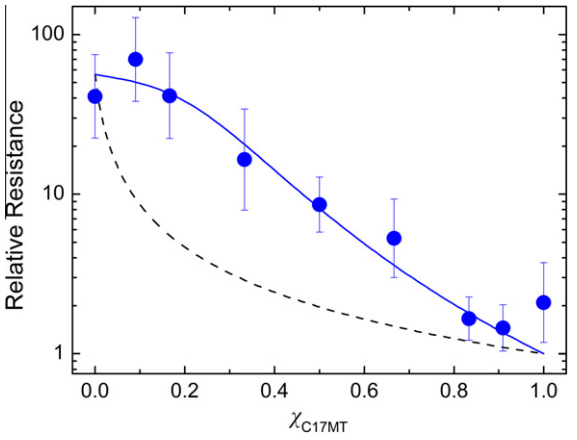

Fig. 5. Relative resistance of binary mixed SAMs of C12 dithiol and C17 monothiol (C12DT and C17MT), as a function of mole fraction of C17MT in solution, χ_{C17MT}, as taken from Fig. 2 and normalized to the end point C17MT. The dashed black line is calculated assuming that all the molecules of each component have the same resistance equal to their resistance in their respective monocomponent SAMs and are connected in parallel in the mixed SAMs. The blue line is calculated by parameterization of the microstructure using Eq. (3). (For interpretation of the references to color in this figure legend, the reader is referred to the web version of this article.)

Another extreme hypothesis would be that molecular composition of the SAM is irrelevant, it just serves as an effective medium (spacer) that only modifies the average width of the tunneling barrier between the contacts. Such a model seems compatible with the exponential dependence on average thickness found. We note that for MT–MT and DT–DT mixed SAMs the slope obtained amounts to 3.54 per fraction. The difference between the end points is six carbon atoms, yielding a slope of 0.6 per carbon atom. Apparently, both systems exhibit the same length dependence with a decay coefficient of about 0.6 per carbon atom. This value corresponds to the one derived in Fig. 1 and to published decay constants for alkane based molecules of 0.5–1.2 [4,6,9]. The resistance changes only due to a different number of carbon atoms, according to Eq. (2), where molecular contribution is given by $r_{mol} \sim exp(\beta n)$, where β is the constant decay coefficient and n in this case is the *average* number of carbon atoms.

Whatever the possible physical justification of this model, not all the observed facts are compatible with it. Note that the absolute value for the resistances of the mixed monothiols is different from that of the mixed dithiols. According to Eq. (2), this offset originates from the different end groups, $-CH_3$ versus –SH, yielding a different top contact contribution, $r_{SAM\ PEDOT}$ [5,6,9,12–14]. The numbers imply a more transparent contact barrier, i.e. a higher transmission coefficient, for the methyl/PEDOT:PSS interface as for the thiol/PEDOT:PSS interface. We note that this behavior is counterintuitive: the water-based suspension PEDOT:PSS is expected to be repelled by the hydrophobic methyl end group of the alkanemonothiols, yielding a less intimate physical contact. Therefore the absolute resistance of a dithiol SAM is expected to be lower than that of a monothiol SAM, contrary to what is experimentally observed; at the moment, we have no explanation for this fact. This difference is significant enough to make certain monocomponent SAMs of longer MT less resistive than those of DT with shorter molecules. Consequently, a systematic resistance *decrease* with *increasing* average layer thickness for certain monothiol–dithiol mixed SAMs (Fig. 3) was observed, which contradicts the effective medium model and stresses the importance of microscopic structure of the junction.

2.3. A phenomenological model for the mixed SAM resistance

The consideration in the previous section demonstrates that a viable model for mixed SAMs should take into account their microstructure in a realistic way, assuming that the resistance can be calculated as for an equivalent circuit of a parallel resistor network. With this in mind, we propose a microdomain model that by parameterization of the microstructure explains the resistance data.

A mixed monolayer is a dynamic system formed at room temperature at relatively low concentrations. Though full phase segregation is thermodynamically favorable, the SAM will nevertheless contain phases with kinetically-formed compositions [15] where domains of different sizes coexist probably even with single molecules. For the purpose of an equivalent circuit of a mixed SAM composed of molecules A and B, we limit the model to four parallel resistances, per molecule: (i) A-domain, (ii) A-single, (iii) B-domain and (iv) B-single. The difference in effective resistance of the same molecule as single or a domain member is supposed to reflect contact and conformational issues, rather than mutual influence of the molecules that we consider irrelevant. Indeed, the longer molecules likely act as pillars and only they are fully contacted by PEDOT:PSS, preventing all short molecules from being equally well contacted and fully contribute to the current. On the other hand, the longer molecules trapped into the shorter molecule domains can hardly stand straight but rather adopt bent conformations. Consequently, "domain" in this context signifies an ensemble of molecules vast enough to be fully contacted (i.e. the fraction of molecules at its boundaries being relatively small), while "singles" might as well apply to groups of a few molecules. Therefore, the resistance of the A and B in domains corresponds to that of the monocomponent SAMs of A and B, respectively, while the resistances of A and B singles have to be parameterized.

We need now a model for the composition of a mixed SAM in terms of domains and singles for both components. It has been known that alkanethiol SAM formation is a two-stage process, the initial fast step being diffusion-limited adsorption and the second slow step reorganization of the primary monolayer described as surface crystallization [16]. For a *mixed* monolayer, we suppose that only a part of the molecules of each type will assemble into domains, while the rest will be in the form of singles. It is reasonable to assume that the shares of the domains and singles depends on the composition of the SAM. Let the molecular composition of the monolayer be characterized by the mole fraction of A denoted by χ; the fraction of B is then $1 - \chi$, $\chi = 0$ corresponds to pure B and $\chi = 1$ corresponds to pure A. When $\chi \to 0$, all molecules B are expected to be organized in domains, while for $\chi \to 1$ practically all

molecules B are single: a view supported by previously reported STM data [17]. We suppose further that a certain number of molecules, n, must meet to form a critical nucleus leading to the formation of a domain, which is more likely to occur when there are more molecules of a given component in the mixed monolayer, hence at a higher mole fraction of this component. Within such a probabilistic approach, the population, of A and B arranged in domains is, χ^n and $(1-\chi)^n$, respectively. The population of singles is then $\chi-\chi^n$ for A and $(1-\chi)$–$(1-\chi)^n$ for B. The resistance of the mixed SAM as a function of composition is then given by:

$$\frac{1}{R}=\frac{\chi^n}{R_{\text{A-domain}}}+\frac{(1-\chi^{n-1})\chi}{R_{\text{A-single}}}+\frac{(1-\chi)^n}{R_{\text{B-domain}}}+\frac{(1-\chi)\left[1-(1-\chi)^{n-1}\right]}{R_{\text{B-single}}} \quad (3)$$

For the mixed SAMs of Fig. 4, the molecule A is C18 monothiol and the molecule B is C12 monothiol. The resistances of the domains, $R_{\text{A-domain}}$ and $R_{\text{B-domain}}$, are taken equal to that of the corresponding end points, *viz.* the pure single component SAMs. As in the case of a perfectly mixed monolayer, the top inset of Fig. 4, we assume that the single molecules C12 monothiol embedded in domains of C18 monothiols, are not contacted by the PEDOT:PSS top contact. Therefore they do not contribute to the overall resistance. Only when organized in sufficiently large domains the short molecules contribute to the overall resistance, as schematically depicted in the lower inset of Fig. 4. The only parameters left are the exponent n and the resistance of a single molecule C18 monothiol in domains of C12 monothiol, $R_{\text{A-single}}$. Fitting the experimental data with Eq. (3) (fully drawn red curve in Fig. 4) yields $n = 2.3$ and $R_{\text{A-single}} = 43$. The resistance of single C18MT molecules in domains of C12MT, $R_{\text{A-single}}$, is in the same order of magnitude as the C18MT domains.

Parameterization of the microstructure can also explain the observed resistance behavior of the mixed C12DT–C17MT system of Fig. 2, where the resistance actually *decreases* with *increasing* average layer thickness. The resistances are replotted in Fig. 5 where the values are normalized to the pure C17MT SAM. Similarly as above, we take the resistances of the domains equal to that of the corresponding end points, the pure monocomponent SAMs. The contribution of the short single molecules is again disregarded. The only parameters left in Eq. (3) are the exponent n and the resistance of a single molecule C17 monothiol in domains of C12 dithiol, $R_{\text{A-single}}$. The dashed black curve in Fig. 4 is calculated assuming that the resistance for single C17MT molecules is the same as that in domains. Contrary to Fig. 4, this assumption does not lead to a fit to the data. This is because C17MT molecules are highly conductive in comparison with C12DT molecules and constitute electric shorts in a C12DT domain. A fitting of both n and $R_{\text{A-single}}$ yields a good agreement, however, with $n = 3.3$ and the relative resistance of the single C17MT molecule equal to 27, an order of magnitude higher than when organized in domains.

This approximately 20-fold increase in the resistance of single long monothiols can be related to their molecular conformation. It has been shown that the resistance of an alkane molecule increases an order of magnitude when gauche defects are introduced [18]. The emergence of defects can be due to conformational disorder, whose origin in a mixed SAM has been described previously [11,15]. Close to the gold surface, the mixed SAM is ordered. The free volume introduced into the outer part of the longer molecules in the monolayer by the presence of the shorter chains makes it disordered and liquid-like. The loss of lateral and orientational order implies the existence of gauche defects.

We note that the degree of conformational disorder in the longer molecules depends on their share in the mixed SAM. At low fraction the gauche densities per molecule are higher [15], meaning that most of the longer molecules exist as singles, in agreement with the assumption that the domain fraction depends on the monolayer composition.

Conformational changes, or gauche defects, affect the charge transport through a molecule directly [18,19], by reducing the periodicity. Indirectly, the resistance can be affected by the presence of bent molecules via altered interface energy of a methyl- to a methylene terminated interface [15,20], as well as by diminishing the electronic coupling of the shorter SAM domains to the top contact [21].

For the monothiol-dithiol SAMs, the presence of gauche defects can be inferred from analysis. On the other hand, conformational disorder in mixed monothiols does not manifest in our electric measurements as the single long molecules already have a higher resistance.

Relatively small values for n support the hypothesis that the dependence of the normalized resistance on the fraction is non-exponential, but follows a power law. Moreover, as simple as our model might be, it embodies some tracts of nucleation and growth phenomena. The assumption of a critical nucleus size of 1–2 molecules might be reasonable [22], although weaker intermolecular interactions can lead to critical nucleus sizes larger than two [23]. The different interactions between the components in the two systems, owing to their different chemical structures, could explain the variation in the value of n. A more rigorous treatment, which would account for the dynamics of the binary SAM in order to relate the trend to the critical nucleus size is beyond the scope of the present work.

3. Synopsis

We have investigated the electrical transport through mixed self-assembled monolayers in large-area molecular junctions. The SAM is formed on a gold bottom electrode inside a photolithographically defined interconnect in photoresist. The conducting polymer PEDOT:PSS is used as top contact. To investigate the contribution of both the length of the molecule and the nature of the end group on the resistance, we systematically studied the charge transport through mixed monolayers of alkanemonothiols and alkanedithiols. We verified by ellipsometry measurements that the segregation coefficient is unity for all investigated binary SAMs. To disentangle the role of the length of the molecule and the interfacial composition we prepared mixed monolayers of all different binary combinations of

two monothiols and two dithiols. The end group is fixed in a series of mixed monothiols and in a series of mixed dithiols.

A trapezoidal correlation in semi-logarithmic resistance-composition coordinates has been obtained (Fig. 3). The straight lines seem to indicate an exponential dependence on composition, or on the average molecular length, also in the case of mono- and dithiol mixed SAMs where resistance can decrease with increasing layer thickness, as the longer component is more conductive in monocomponent SAM. However mathematically simple, exponential dependence is difficult to justify physically for mixed monolayers, unlike the case of monocomponent SAMs where this dependence has a single-molecule tunneling origin.

We search for the origin of the resistance-composition dependence in mixed SAMs in an equivalent circuit model based on their microdomain structure for which we suggest a simple model. In essence, we suppose that the effective resistance of a molecule can differ depending on whether it is isolated (that is, trapped within an alien molecular domain) or belongs to a domain of the same molecules, due to contact and conformational issues. The simulated dependence is non-exponential and leads to a good agreement between calculated and measured resistances with only two fit parameters.

4. Experimental section

A 4-in. silicon wafer with a 500 nm thermally grown oxide was passivated using hexamethyldisilazane (HMDS). A 1 nm layer of chromium was thermally evaporated through a shadow mask, followed by 60 nm of gold. The rms roughness of the bottom contact is about 0.7 nm over an area of 0.25 μm^2.

The two terminal junctions were photolithographically defined in an insulating matrix of photoresist, ma-N 1410 (Micro Resist Technology GmbH). The negative photoresist was spincoated on the wafer resulting in a layer of 570 nm. After a pre-bake step to remove any remaining solvents, the layer was exposed to UV light with a Karl Süss MA1006 mask aligner, to define the vertical interconnects, ranging from 5 to 100 μm in diameter. After development, the film was hard baked at 200 °C for at least 1 h to render the photoresist insoluble in ethanol, the solvent used in the SAM formation. The wafer was subsequently cut in several pieces using a diamond tip pen. This allowed the simultaneous processing of different mixed SAMs on a single wafer, thereby eliminating processing variations that can affect device performance. A last step before self-assembly was cleaning of the bottom gold contacts with a PDC plasma cleaner (Harrick plasma) to remove any photoresist residuals.

The self-assembled monolayers were formed from molecules dissolved in ethanol. The series of molecules used in this work include 1-dodecanethiol (C12MT), 1-heptadecanethiol (C17MT), 1-octadecanethiol (C18MT), 1-eicosanethiol (C20MT), 1,12-dodecanedithiol (C12DT) and 1,16-hexadecanedithiol (C16DT). All solvents and molecules except C17MT, C20MT, C12DT and C16DT were purchased from Sigma–Aldrich. The synthesis of the other molecules was performed starting from the carboxylic acid, hydroxyl or bromide precursor, depending on the commercially available compounds.

Mixed solutions of various molar ratios between the two components were prepared by mixing stock solutions of each component at the appropriate volume ratio. The wafer pieces were immersed in the solutions for at least 36 h, under nitrogen. The concentration in ethanol was 3×10^{-3} M for the C12DT–C17MT system, 6×10^{-3} M for the C12MT–C18MT systems and 1×10^{-2} M for the mixed SAMs of Fig. 3. The higher concentration is required to prevent formation of a looped phase when using longer alkanedithiols (C16DT) [24]. After the self-assembly, the wafer pieces were thoroughly rinsed with ethanol, toluene and *iso*-propanol to remove any remaining alkanethiol molecules.

Subsequently, the interlayer of PEDOT:PSS, a water-based suspension of poly(3,4-ethylenedioxythiophene) and poly(4-styrenesulphonic acid), was spin coated. PEDOT:PSS acts as a highly conductive buffer layer that protects the SAM during subsequent evaporation of the top gold contact. Two blends were used. (a) Baytron® PH500, H.C. Starck GmbH & Co., filtered over a 1 μm Whatman® glass filter. Dimethylsulfoxide (5% v/v) was added to increase the conductivity [25] and (b) AGFA® ICP new type filtered over a 5 μm Whatman® glass filter. Blend (a) was used for the C12MT–C18MT system, while blend (b) was used for all other experiments. The PEDOT:PSS solution was spincoated, resulting in a layer thickness of about 90 nm. The wafer was then immediately transferred to a vacuum oven for at least 1 h to dry the film.

To facilitate contacting the top electrode, 100 nm of gold was evaporated through a shadow mask. This gold layer, apart from ensuring a better contact with the measurement probes, also serves as a self aligned mask for the removal of redundant PEDOT:PSS by reactive ion etching (O_2 plasma). This step eliminates any parasitic currents from top to bottom electrode.

Current–voltage (*I–V*) measurements were performed in two home-built probe stations using a Keithley 4200 Semiconductor Analyzer Characterization System. The probe stations were pressurized at 10^{-6}–10^{-7} mbar for at least 6 h before the measurements, to remove any water absorbed in the PEDOT:PSS layer. Devices were swept in the voltage range of 0 to 1 to −1 V and back to 0 V and the recorded current densities were averaged for all devices with different diameter. The normalized resistance (*RS*, resistance × area, $\Omega\,\mu m^2$) was then calculated at 0.1 V bias. The resistance scales linearly with device area for junctions of 5–100 μm in diameter, resulting in identical *RS* values.

Ellipsometric measurements, to verify that the segregation coefficient is unity and that the layer thickness linearly increases with composition, were performed using a V-VASE® ellipsometer (J.A. Woolam Co., Inc.) equipped with an HS-190 high speed monochromatic system and controlled with a VB-400 module. All measurements were performed at the reflection geometry in the spectral range from 350 to 500 nm with a step of 3 nm, at an angle of incidence of 65–75° with a step of 5° and 10 revisions/measurement. Acquired data were analyzed using WVASE32® software. The index of refraction for monothiols and

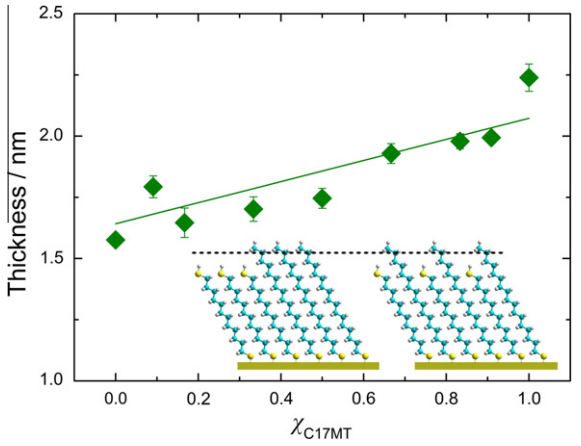

Fig. 6. The thickness obtained from ellipsometry measurements on binary mixed SAMs of C12 dithiol and C17 monothiol (C12DT and C17MT), as a function of the fraction C17MT in solution, χ_{C17MT}. The fully drawn curve is a linear extrapolation between the end points, which have been calculated using Hyperchem 7.5.

dithiols was taken equal as 1.45. The layer thickness derived as a function of composition in solution for the C12DT–C17MT mixed SAMs is presented in Fig. 6. A linear dependence is found indicating that within experimental error the segregation coefficient is unity, as has been reported previously [26]. This conclusion is substantiated by the calculated layer thicknesses indicated by the fully drawn curve. The end points follow from the length of the molecule, calculated with Hyperchem 7.5, adding 2.3 Å for the S–Au bonds and taking an off-normal tilt angle of 30°. The fully drawn curve is obtained by a linear extrapolation between the end points and fits the data well. This analysis applies for all binary SAMs here investigated.

For the sample preparation, a silicon wafer with 500 nm thermally grown oxide was rinsed with *iso*-propanol, dried in a dry spinner and coated with 1 nm Cr adhesion layer and 60 nm of Au, according to the procedure described above. The wafer was cut to pieces, which were transferred in nitrogen filled bottles for the ellipsometry measurements (one reference point per piece). Subsequently, the pieces were treated in a plasma cleaner and immersed in the respective solutions to self-assemble the monolayers. Ellipsometry samples and molecular junctions were prepared simultaneously from the same solutions. The thickness of the SAMs was determined by averaging at least three different measurements on each piece.

Acknowledgements

The authors thank P.A. van Hal and E.H. Huisman for stimulating discussions, and J. Harkema and F. van der Horst for technical support. We are grateful to an anonymous referee for his/her valuable comments and suggestions. We acknowledge financial support from the Zernike Institute for Advanced Materials, the European Community's Seventh Framework Programme (FP7/2007–2013) under the Grant agreements ONE-P No. 212311, the Interuniversity Attraction Pole IAP 6/27 Program of the Belgian Federal Government, and NanoNed, a national nanotechnology program coordinated by the Dutch Ministry of Economic Affairs.

References

[1] (a) J.C. Love, L.A. Estroff, J.K. Kriebel, R.G. Nuzzo, G.M. Whitesides, Chem. Rev. 105 (2005) 1103–1170 (and references therein);
(b) M.D. Porter, T.B. Bright, D.L. Allara, C.E.D. Chidsey, J. Am. Chem. Soc. 109 (1987) 3559–3568;
(c) C. Vericat, M.E. Vela, G.A. Benitez, J.A.M. Gago, X. Torrelles, R.C. Salvarezza, J. Phys.: Condens. Matter 18 (2006) R867–R900.
[2] (a) P.E. Laibinis, G.M. Whitesides, J. Am. Chem. Soc. 114 (1992) 1990–1995;
(b) A. Ulman, S.D. Evans, Y. Shnidman, R. Sharma, J.E. Eilers, J.C. Chang, J. Am. Chem. Soc. 113 (1991) 1499–1506;
(c) C. Pale-Grosdemange, E.S. Simon, K.L. Prime, G.M. Whitesides, J. Am. Chem. Soc. 113 (1991) 12–20;
(d) D.L. Allara, A.F. Heburd, F.J. Padden, R.G. Nuzzo, D.R. Falcon, J. Vac. Sci. Technol. A 1 (1983) 376–382;
(e) V. DePalma, N. Tillman, Langmuir 5 (1989) 868–872;
(f) C.E.D. Chidsey, Science 251 (1991) 919–922;
(g) G.K. Rowe, S.E. Creager, Langmuir 7 (1991) 2307–2312;
(h) B. de Boer, A. Hadipour, M.M. Mandoc, T. van Woudenbergh, P.W.M. Blom, Adv. Mater. 17 (2005) 621–625.
[3] (a) G.K. Ramachandran, T.J. Hopson, A.M. Rawlett, L.A. Nagahara, A. Primak, S.M. Lindsay, Science 300 (2003) 1413–1416;
(b) A.S. Blum, J.G. Kushmerick, D.P. Long, C.H. Patterson, J.C. Yang, J.C. Henderson, Y. Yao, J.M. Tour, R. Shashidhar, B.R. Ratna, Nat. Mater. 4 (2005) 167–172;
(c) Z.J. Donhauser, B.A. Mantooth, T.P. Pearl, K.F. Kelly, S.U. Nanayakkara, P.S. Weiss, Jpn. J. Appl. Phys. 41 (2002) 4871–4877.
[4] H.B. Akkerman, P.W.M. Blom, D.M. de Leeuw, B. de Boer, Nature 441 (2006) 69–72.
[5] T.W. Kim, G. Wang, H. Lee, T. Lee, Nanotechnology 18 (2007) 315204. p. 8.
[6] P.A. van Hal, E.C.P. Smits, T.C.T. Geuns, H.B. Akkerman, B.C. de Brito, S. Perissinotto, G. Lanzani, A.J. Kronemeijer, V. Geskin, J. Cornil, P.W.M. Blom, B. de Boer, D.M. de Leeuw, Nat. Nanotechnol. 3 (2008) 749–754 (including supporting info).
[7] G. Wang, T.-W. Kim, H. Lee, T. Lee, Phys. Rev. B 76 (2007) 205320. p. 7.
[8] A.J. Kronemeijer, E.H. Huisman, I. Katsouras, P.A. van Hal, T.C.T. Geuns, P.W.M. Blom, S.J. van der Molen, D.M. de Leeuw, Phys. Rev. Lett. 105 (2010) 156604. p. 4.
[9] H.B. Akkerman, B. de Boer, J. Phys.: Condens. Matter 20 (2008) 013001 (p. 20, and references therein).
[10] (a) S. Chen, L. Li, C.L. Boozer, S. Jiang, Langmuir 16 (2000) 9287–9293;
(b) K. Heister, D.L. Allara, K. Bahnck, S. Frey, M. Zharnikov, M. Grunze, Langmuir 15 (1999) 5440–5443.
[11] C.D. Bain, G.M. Whitesides, J. Am. Chem. Soc. 111 (1989) 7164–7175.
[12] J.M. Seminario, L. Yan, Int. J. Quantum Chem. 102 (2005) 711–723.
[13] (a) H. Haick, O. Niitsoo, J. Ghabboun, D. Cahen, J. Phys. Chem. C 111 (2007) 2318–2329;
(b) F. Chen, X. Li, J. Hihath, Z. Huang, N. Tao, J. Am. Chem. Soc. 128 (2006) 15874–15881;
(c) B. Kim, J.M. Beebe, Y. Jun, X.Y. Zhu, C.D. Frisbie, J. Am. Chem. Soc. 128 (2006) 4970–4971.
[14] (a) F. Tao, S.L. Bernasek, Chem. Rev. 107 (2007) 1408–1453 (and references therein);
(b) P.E. Laibinis, G.M. Whitesides, D.L. Allara, Y.-T. Tao, A.N. Parikh, R.G. Nuzzo, J. Am. Chem. Soc. 113 (1991) 7152–7167;
(c) H. Basch, R. Cohen, M.A. Ratner, Nano Lett. 5 (2005) 1668–1675;
(d) X. Li, J. He, J. Hihath, B. Xu, S.M. Lindsay, N. Tao, J. Am. Chem. Soc. 128 (2006) 2135–2141.
[15] P.E. Laibinis, R.G. Nuzzo, G.M. Whitesides, J. Phys. Chem. 96 (1992) 5097–5105.
[16] A. Ulman, Chem. Rev. 96 (1996) 1533–1554.
[17] G.E. Poirier, Chem. Rev. 97 (1997) 1117–1127.
[18] (a) C. Li, I. Pobelov, T. Wandlowski, A. Bagrets, A. Arnold, F. Evers, J. Am. Chem. Soc. 130 (2008) 318–326;
(b) M. Fujihira, M. Suzuki, S. Fujii, A. Nishikawa, Phys. Chem. Chem. Phys. 8 (2006) 3876–3884.
[19] (a) M. Paulsson, C. Krag, T. Frederiksen, M. Brandbyge, Nano Lett. 9 (2009) 117–121;
(b) K. Tagami, M. Tsukada, e-J. Surf. Sci. Nanotechnol. 2 (2004) 186–190.

[20] A. Ulman, An Introduction to Ultrathin Organic Films: From Langmuir-Blodgett to Self-Assembly, Academic Press, Inc., San Diego, 1991. pp. 48–58.
[21] R.L. York, K. Slowinski, J. Electroanal. Chem. 327 (2003) 550–551.
[22] I. Doudevski, D.K. Schwartz, Phys. Rev. B 60 (1999) 14–17.
[23] (a) M. Brinkmann, S. Graff, F. Biscarini, Phys. Rev. B 66 (2002) 165430. p. 11;
(b) S. Verlaak, S. Steudel, P. Heremans, D. Janssen, M.S. Deleuze, Phys. Rev. B 68 (2003) 195409. p. 8.
[24] H.B. Akkerman, A.J. Kronemeijer, P.A. van Hal, D.M. de Leeuw, P.W.M. Blom, B. de Boer, Small 4 (2008) 100–104.
[25] J.Y. Kim, J.H. Jung, D.E. Lee, J. Joo, Synth. Met. 126 (2002) 311–316.
[26] J.P. Folkers, P.E. Laibinis, G.M. Whitesides, Langmuir 8 (1992) 1330–1341.